Electronic Structures and Spectra of Aminoacetophenones and Related Compounds

Ryoichi NAKAGAKI,† Saburo NAGAKURA,*,†,†† Takayoshi KOBAYASHI,†† and Suehiro IWATA††

†*The Institute for Solid State Physics, The University of Tokyo, Minato, Tokyo 106*

††*The Institute of Physical and Chemical Research, Wako, Saitama 351*

(Received June 10, 1978)

The $S_n \leftarrow S_0$ and $S_n \leftarrow S_1$ transition bands were measured with *m*- and *p*-dimethylaminoacetophenones and related compounds in order to clarify the characters of the excited singlet states. The observed spectra were reasonably interpreted by the use of the theoretical results based on the composite molecule method. The longest wavelength band ($S_1 \leftarrow S_0$) of the meta isomer has mainly the local excitation (LE) character of aniline ($^1B_2 \leftarrow {}^1A_1$), while that of the para isomer is ragarded as the intramolecular charge-transfer band. In the para isomer the LE transition corresponding to $^1B_2 \leftarrow {}^1A_1$ is covered by the intense CT band. The $S_n \leftarrow S_1$ transitions of the meta isomer are almost of LE character, whereas those of the para isomer are of back CT nature. This is mainly attributed to the difference in the character of S_1.

The π-electron systems of organic compounds containing electron donor and electron acceptor group have been extensively studied from the standpoint of intramolecular charge-transfer interaction.[1-13] Disubstituted benzene molecules, D–C_6H_4–A, where D and A represent an electron donor and an electron acceptor, respectively, are typical intramolecular donor-acceptor systems and exhibit characteristic absorption spectra. The spectra have been interpreted by the composite molecule method (the molecules in molecule method) for nitroanilines, nitrophenols, cyanophenols, and other compounds.[4,7,14,15] More recently, McGlynn and coworkers studied the luminescence spectra and kinetic parameters of cyanoanisoles, fluorobenzonitriles, cyanoanilines, and nitroanilines.[16-18] The $T_n \leftarrow T_1$ transitions of aminobenzenes and cyanobenzenes were measured and discussed in terms of intramolecular charge-transfer interaction.[19,20]

In the present work, the $S_n \leftarrow S_0$ and $S_n \leftarrow S_1$ (transient) absorption spectra of aminoacetophenones and related compounds have been measured in order to clarify the characters of the excited states. The $S_n \leftarrow S_0$ and $S_n \leftarrow S_1$ transitions of aminoacetophenones were analyzed with the aid of the theoretical results based on the composite molecule method, in which the intramolecular charge-transfer interaction of the aminophenyl group with the carbonyl group was considered.

Experimental

Materials. Commercially available *m*- and *p*-aminoacetophenones (*m*- and *p*-AAP), *p*-dimethylaminobenzaldehyde (*p*-DMABA), *N*,*N*-dimethyl-*p*-nitroaniline (*p*-DMNA) were chromatographed from benzene on activated alumina and recrystallized from the same solvent. The meta and para isomers of dimethylaminoacetophenone (*m*- and *p*-DMAAP) and *p*-dimethylaminobenzonitrile (*p*-DMABN) were synthesized according to the methods described in literature,[21-23] and purified in the same manner as mentioned above.

Measurements. Visible and ultraviolet absorption spectra were measured on a Cary 14 recording spectrophotometer. Emission spectra were measured with a Spex 1700-II grating monochromator equipped with an EMI 6256S photomultiplier and a PAR 128 lock-in amplifier. The fluorescence quantum yield was determined by the use of a Shimadzu RF-502 spectrofluorometer, 2,5-diphenyloxazole with the quantum yield of 1.00 in cyclohexane[24] being used as the standard. A method for the determination of fluorescence lifetimes was the same as described previously.[25]

For the measurement of transient absorption spectra two methods were employed; the one is an ordinary N_2 laser photolysis method (method I), the details of which were already reported,[25] and the other is a method using superradiant fluorescence from solution as an analyzing light source (method II).[26] The transient absorption spectra obtained by the latter method were superposition of the $S_n \leftarrow S_1$ and $T_n \leftarrow T_1$ transitions. Even for fluorescent compounds method II is applicable to the measurement of the $S_n \leftarrow S_1$ transition bands. In method II, dyes used were as follows: 3-cyano-7-hydroxy-4-methylcoumarin, coumarin 1 (7-dimethylamino-4-methylcoumarin), coumarin 30 (3-(2′-methyl-1-benzimidazolyl)-7-diethylaminocoumarin), 7-diethylamino-4-(trifluoromethyl)-coumarin, Brilliant Sulfaflavine, Uranine, Rhodamine 6G, Rhodamine B, Cresyl Violet perchlorate–Rhodamine 6G mixture, and Cresyl Violet perchlorate–Rhodamine B mixture.

For the measurement of the transient absorption spectra the concentration of the solution was adjusted so that the absorbance at 337.1 nm was $\approx$1.0 in 1 mm light-path.

Theoretical

Molecular Geometry of Aminoacetophenones. In carrying out the MO calculations on aminoacetophenones the following assumptions were made concerning the molecular geometry; the molecules are planar, the phenyl rings are equilateral hexagonals with the C–C distance of 1.397 Å,[27] and the angle between the double bond of the carbonyl group and the single bond linked to the phenyl ring is 120°. Other atomic distances were taken from the data on *p*-aminoacetophenone determined by X-ray crystal analysis:[28] namely, the C–C distance in the single bond between the carbonyl and the phenyl group is 1.468 Å, the C–O distance in the carbonyl double bond is 1.215 Å, and the C–N distance is 1.376 Å.

Configuration Interaction Calculation. In the present treatment aminoacetophenones are considered to be composite molecules consisting of an electron donor, aminophenyl group, and an electron acceptor, carbonyl group. The π-electron energy and wave functions of several electron configurations; the ground (G) configuration, the locally excited (LE) configura-

tions within the aminophenyl group, and the charge-transfer (CT) configurations in which an electron in the occupied orbital of the donor is transferred into the anti-bonding orbital of the acceptor. The diagonal energies corresponding to the local excitations of aminophenyl group were taken from the spectroscopic data on anilines and *N*-alkylated derivatives in the previous paper.[9]

To evaluate the off-diagonal elements between LE and CT configurations, the accurate wave functions for the LE's of aminophenyl groups were required. At first, the LCAO SCF MO's of the π-electron systems of aniline and *N*,*N*-dimethylaniline, $\phi_i (i=1\text{—}7)$, were calculated by the aid of the Pariser-Parr-Pople method.[29] The wave functions for the ground and excited states of aniline and *N*,*N*-dimethylaniline were obtained by considering CI among electron configurations constructed from the SCF MO's. The configurations considered in the CI calculation are given below: for A_1 symmetry, 28 configurations, that is, the ground, 5 singly excited, 14 doubly excited, and 8 triply excited configurations, and for B_2 symmetry, 25 configurations, that is, 5 singly excited, 12 doubly excited, and 8 triply excited configurations. From the resultant excited wave functions the lowest 3 wave functions with A type symmetry and the lowest 3 wave functions with B type symmetry were picked up as LE configurations for the further CI calculations of energy levels and wave functions of aminoacetophenones.

The molecular orbitals of the carbonyl group obtained by Tanaka were used in the present calculation.[30]

The CT configurations taken in the CI calculation for aminoacetophenones were given below:

$$\text{CT(4-A)} = (\phi_4^{-1}\text{A}),\ \text{CT(3-A)} = (\phi_3^{-1}\text{A}),\ \text{and}$$
$$\text{CT(2-A)} = (\phi_2^{-1}\text{A}).$$

Here, A denotes the anti-bonding orbital of the acceptor, carbonyl group, and ϕ_i the *i*-th occupied orbital of aniline, the highest occupied orbital being ϕ_4. The energies of the CT configurations were evaluated by the equation,

$$E(\text{CT}) = I_{\text{P}}(\phi_i) - E_{\text{A}}(\text{C=O}) - C,$$

where $I_{\text{P}}(\phi_i)$ is the ionization potential of the donor, E_{A}(C=O) is the electron affinity of the acceptor, and C is the coulombic interaction energy between the donor and acceptor groups. The values of I_{P} were taken from the photoelectron spectroscopic data,[31,32] the affinity E_{A} was assumed as -1.2 eV,[5] and C values were calculated by using the values of two center Coulomb repulsion integrals (rr|ss), which were evaluated according to the Pariser-Parr method.[29]

The off-diagonal matrix elements of the total electronic Hamiltonian were evaluated by the aid of the formulations by Pople[33] and by Longuet-Higgins and Murrell.[3] They were given in terms of $\beta_{\text{C-C=O}}$, the core resonance integral between the ring carbon and the carbonyl carbon. Actual calculations were made by changing $\beta_{\text{C-C=O}}$ as a parameter from -1.50 eV to -1.90 eV by a step of 0.10 eV. Consequently, the results were found to be insensitive to the parameter. The energies and wave functions for $\beta_{\text{C-C=O}}$ of -1.90 eV are shown in Table 1.

Table 1. The energy levels and wave functions of *m*- and *p*-dimethylaminoacetophenone

(*m*-DMAAP)

$W_0 = -0.23$ eV

$\Psi_0 = -0.9815\Psi_{\text{G}} + 0.1398\Psi_{\text{CT(4-A)}} + 0.1129\Psi_{\text{CT(2-A)}} + \cdots$

$W_1 = 3.87$ eV

$\Psi_1 = -0.7615\Psi_{^1\text{B}_2} + 0.6044\Psi_{\text{CT(4-A)}} + 0.1960\Psi_{^2\text{A}_1} + \cdots$

$W_2 = 4.77$ eV

$\Psi_2 = 0.5965\Psi_{^1\text{B}_2} + 0.5783\Psi_{^2\text{A}_1} + 0.5427\Psi_{\text{CT(4-A)}} + \cdots$

$W_3 = 5.34$ eV

$\Psi_3 = 0.6924\Psi_{^2\text{A}_1} - 0.5306\Psi_{\text{CT(4-A)}} + 0.4145\Psi_{\text{CT(3-A)}} - 0.2017\Psi_{^1\text{B}_2} + \cdots$

$W_4 = 5.63$ eV

$\Psi_4 = 0.7203\Psi_{\text{CT(3-A)}} - 0.4098\Psi_{^2\text{B}_2} - 0.3706\Psi_{^2\text{A}_1} + 0.3133\Psi_{^3\text{A}_1} + \cdots$

(*p*-DMAAP)

$W_0 = -0.28$ eV

$\Psi_0 = -0.9747\Psi_{\text{G}} - 0.1821\Psi_{\text{CT(4-A)}} - 0.1278\Psi_{\text{CT(2-A)}} + \cdots$

$W_1 = 4.17$ eV

$\Psi_1 = 0.8049\Psi_{\text{CT(4-A)}} - 0.5635\Psi_{^2\text{A}_1} - 0.1514\Psi_{\text{G}} + \cdots$

$W_2 = 4.25$ eV

$\Psi_2 = -0.9822\Psi_{^1\text{B}_2} + 0.1799\Psi_{\text{CT(3-A)}} + \cdots$

$W_3 = 5.57$ eV

$\Psi_3 = 0.7403\Psi_{\text{CT(3-A}} + 0.6463\Psi_{^2\text{B}_2} + 0.1712\Psi_{^1\text{B}_2} + \cdots$

$W_4 = 5.61$ eV

$\Psi_4 = 0.8250\Psi_{^2\text{A}_1} + 0.5531\Psi_{\text{CT(4-A)}} + \cdots$

G, the ground configuration; $n\text{A}_1$, the *n*-th LE of aniline with A_1 symmetry ($n \geq 2$); $m\text{B}_2$, the *m*-th LE of aniline with B_2 symmetry ($m \geq 1$); CT(*i*-A), CT from the *i*-th MO of aniline to acceptor.

The oscillator strengths were calculated by the use of the equation,

$$f = 8.753 \times 10^{-2} Q^2 \Delta E,$$

where $Q = (\Psi_0 | \boldsymbol{er} | \Psi_1)$, and ΔE is the transition energy in eV. The theoretical results of the transition energies and oscillator strengths are shown in Table 2, together with the observed values.

Table 2. Transition energies (ΔE (eV)) and oscillator strengths (f) observed and calculated for the meta and para isomers of dimethylamino-acetophenone

Transition	Calcd		Obsd		
	ΔE	f	$\Delta E^{a)}$	$f^{a)}$	$\Delta E^{b)}$
(*m*-DMAAP)					
$\Psi_1 \leftarrow \Psi_0$	4.10	0.028	3.51	0.046	
$\Psi_2 \leftarrow \Psi_0$	5.00	0.099	4.79	0.13	
$\Psi_3 \leftarrow \Psi_0$	5.57	0.186	5.18	0.49	
$\Psi_4 \leftarrow \Psi_0$	5.86	0.018	>5.58		
(*p*-DMAAP)					
$\Psi_1 \leftarrow \Psi_0$	4.45	0.076	3.97	(0.46)	3.49
$\Psi_2 \leftarrow \Psi_0$	4.53	0.028			≈ 4.1
$\Psi_3 \leftarrow \Psi_0$	5.85	0.225	5.33	(0.13)	≈ 5.0
$\Psi_4 \leftarrow \Psi_0$	5.88	0.682			≈ 5.4

a) In cyclohexane. b) In 1,1,1,3,3,3-hexafluoro-2-propanol (HFP).

Results and Discussion

The $S_n \leftarrow S_0$ Transition Bands of m- *and* p-*Dimethylaminoacetophenones.* In cyclohexane, the $n\pi^*$ band of *m*-DMAAP or *p*-DMAAP was observed as a weak tail (log $\varepsilon \leq 2$) at the longer wavelength side of the lowest $\pi\pi^*$ or CT band. In polar solvents, however, it was found to be covered by the intense $\pi\pi^*$ or CT band.

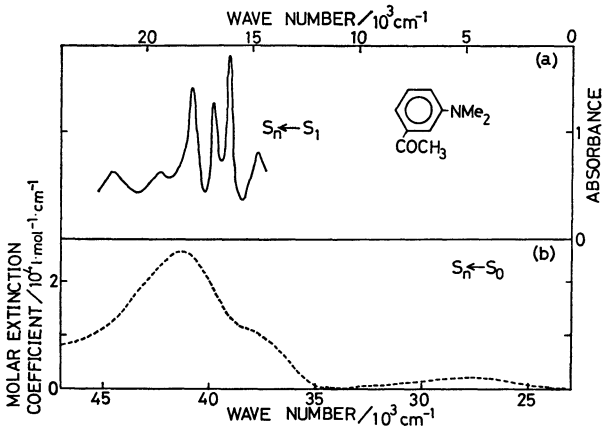

Fig. 1. (a) Upper: the transient absorption spectrum of *m*-DMAAP in ethanol at room temperature obtained by method II. The transition energy is indicated on the upper abscissa in the units of 1000 cm^{-1}. (b) Lower: the absorption spectrum of *m*-DMAAP in ethanol at room temperature. The transition energy is indicated on the lower abscissa in the units of 1000 cm^{-1}.

In the absorption spectrum of ethanolic solution of *m*-DMAAP (Fig. 1-b), we can see four $\pi\pi^*$ transition bands: three bands at 27600, 37800, and 41300 cm^{-1} and an additional tail at higher energy side (45000 cm^{-1}). In cyclohexane solution of *p*-DMABA or *p*-DMAAP (Fig. 3 or 4), two bands were observed in the region, 28000—47000 cm^{-1}.

The intense long wavelength band of *p*-DMAAP or *p*-DMABA shows the increasing red-shift on going from the nonpolar solvent, cyclohexane, to the polar ones: cyclohexane<acetonitrile<ethanol<water<1, 1, 1, 3, 3,-3,-hexafluoro-2-propanol (HFP) (see Figs. 2-b, 4, and 5). The largest red-shift was observed in HFP solution, in spite of the rather low dielectric constant and refractive index of this solvent (16.62 at 25 °C and 1.2750 at Na D line) compared with those of ethanol (24.3 and 1.3618), acetonitrile (37.5 and 1.3437), and water (78.54 and 1.3330). This fact indicated that the red-shift observed in HFP is mainly due to hydrogen bonding.[34] In the HFP solution of *p*-DMAAP or *p*-DMABA, four $\pi\pi^*$ or CT bands were observed: *e.g.* for *p*-DMABA, one strong band at 27400, and three bands at $\approx$33000, $\approx$39800, and $\approx$43500 cm^{-1} (Fig. 3). Formation of strong hydrogen bonds between the solute, *p*-DMAAP or *p*-DMABA, and the solvent, HFP, causes the large red-shift of some of the absorption bands. On the other hand, the bands less sensitive to the hydrogen bonding show small solvent shift. As the result the two bands observed in cyclohexane split into four components in strongly hydrogen bonding HFP.

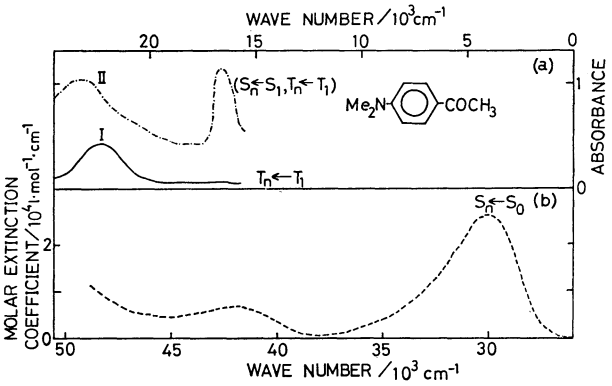

Fig. 2. (a) Upper: I, the $T_n \leftarrow T_1$ transition spectrum of *p*-DMAAP in ethanol at room temperature obtained by method I. II, the transient absorption spectrum of *p*-DMAAP in ethanol at room temperature obtained by method II. The transition energy is indicated on the upper abscissa in the units of 1000 cm^{-1}. (b) Lower: the absorption spectrum of *p*-DMAAP in ethanol at room temperature. The transition energy is indicated on the lower abscissa in the units of 1000 cm^{-1}.

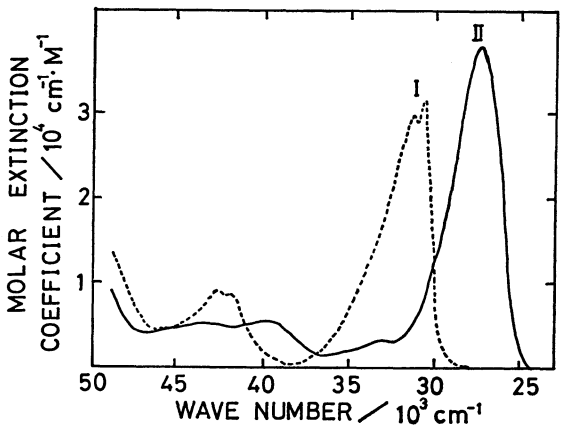

Fig. 3. The absorption spectrum of *p*-DMABA at room temperature. I: in cyclohexane, II: in HFP.

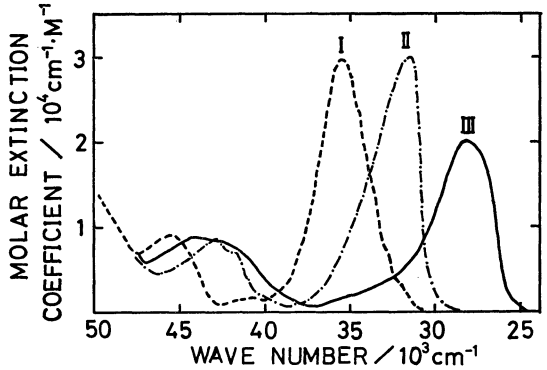

Fig. 4. The absorption spectra in cyclohexane at room temperature.
I: *p*-DMABN, II: *p*-DMAAP, and III: *p*-DMNA.

The energy levels calculated for *m*- and *p*-DMAAP with and without CI are shown in Fig. 6. The calculations predict four transitions for *m*-DMAAP and *p*-DMAAP below 6 eV and can explain the observed

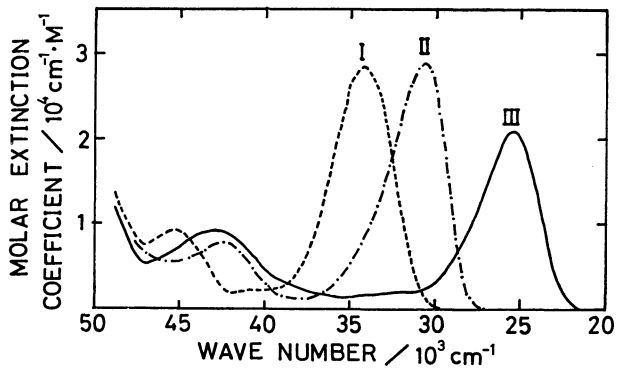

Fig. 5. The absorption spectra in acetonitrile at room temperature.
I: *p*-DMABN, II: *p*-DMAAP, and III: *p*-DMNA.

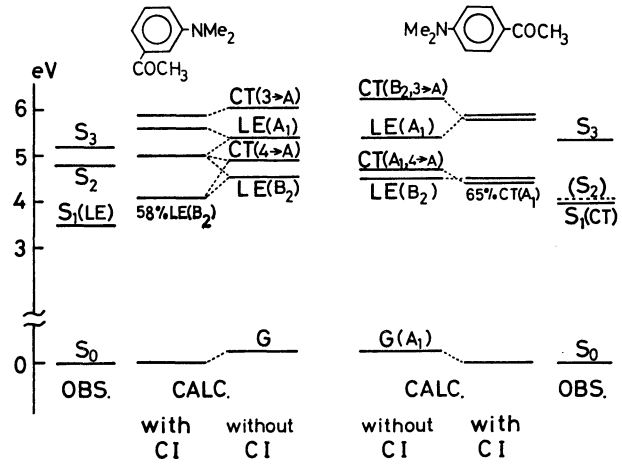

Fig. 6. Energy levels of *m*-DMAAP and *p*-DMAAP with and without CI.

results at least semi-quantitatively (see Table 2).

The S_n←S_1 Transitions of m- *and* p-*Dimethylaminoacetophenones.* The transient absorption spectrum of *m*-DMAAP is given in Fig. 1, together with the S_n←S_0 spectrum. The T_n←T_1 transition of *m*-DMAAP was not detected by method I in the region, 14300—27800 cm^{-1}. Therefore, the transient absorption spectrum obtained by method II is purely attributed to the S_n←S_1 transitions. From the consideration of the observed frequencies of the S_n←S_0 transition bands, the S_n←S_1 band at 17000 cm^{-1} is safely assigned to the S_3←S_1 transition. This band shows vibrational structures, suggesting that this transition is largely of forbidden character. The oscillator strength of the S_3←S_1 transition was calculated to be 0.07, by assuming that the molecular geometry in the excited state is the same as that in the ground state. This theoretical prediction is consistent with the observed result.

The transient spectra of *p*-DMAAP are given in Fig. 2-a. Very similar transient spectra are also obtained for *p*-DMABA. The T_n←T_1 spectrum of *p*-DMAAP was observed by method I, and the transient spectrum measured by method II was found to be composed of the S_n←S_1 and the T_n←T_1 transition bands. The S_n←S_1 transition band appears at 16700 cm^{-1} for *p*-DMAAP and may be assigned to the S_3←S_1 or S_4←S_1 transitions from the consideration of the observed frequencies of the S_n←S_0 transition bands of *p*-DMAAP (Table 2). The oscillator strength was evaluated to be 0.03 and 0.50 for the S_3←S_1 and S_4←S_1 transitions, respectively, in the same assumption as mentioned above. Hence, the S_4←S_1 assignment was preferred.

The Characters of the Lowest Excited Singlet States of m- *and* p-*Dimethylaminoacetophenones.* The kinetic parameters for the lowest excited singlet states were determined in EPA (5:5:2) at 77 K. The results are as follows: for *m*-DMAAP, τ_f(fluorescence lifetime)=54 ns and ϕ_f(fluorescence quantum yield)=0.85, and for *p*-DMAAP, τ_f=3.5 ns and ϕ_f=0.64. From these values the fluorescence radiative rate constants are calculated to be 1.7×10^7 s^{-1} for *m*-DMAAP, and 1.8×10^8 s^{-1} for *p*-DMAAP. This fact, together with the spectral difference between the absorptions of *m*-DMAAP and *p*-DMAAP (lower figures of Figs. 1 and 2) shows that the lowest excited states of both isomers have different electronic structures. According to the present theoretical consideration, the longest wavelength band of *m*-DMAAP originates mainly from the local excitation of aniline ($^1B_2$←$^1A_1$), while that of *p*-DMAAP or *p*-DMABA is assigned as the CT band which is associated with the charge-transfer configuration (ϕ_4←^1A). The theoretical result is supported by the fact that the longest wavelength band of *p*-DMAAP or *p*-DMABA has the transition moment nearly parallel to the molecular long axis.[35] Thus it is concluded that the S_1 state of the meta-isomer has the LE character within *N,N*-dimethylaniline, while that of the para-isomer the CT character.

Let us consider the spectral difference in the S_n←S_1 transitions between the meta- and para-isomers on the basis of the above-mentioned nature of the S_1 states. The final states of the S_n←S_1 transition bands, S_3 of the meta-isomer and S_4 of the para-isomer are nearly of the same nature: LE of *N,N*-dimethylaniline ($^1A_1$←$^1A_1$) perturbed by CT(4-A). Hence, the S_n←S_1 transition band can be interpreted as the LE band for the meta-isomer and as the back CT band for the para-isomer.

The Characters of Lower-lying Excited States of Several Related Aniline Derivatives. The spectra of dimethylaminoacetophenones are correlated with those of aminoacetophenones and other aniline derivatives containing various acceptor groups.

The two isomers of aminoacetophenone, *m*-AAP and *p*-AAP exhibit absorption spectra similar to those of the corresponding *N,N*-dimethylated compounds, *m*-DMAAP and *p*-DMAAP. Concerning the S_1←S_0 transition, the decrease of the transition energy and the increase of the oscillator strength were observed alkylation of the amino group. This observation is reasonably interpreted in terms of the CT interaction. The red-shift and intensification of the longest wavelength band due to alkylation can be interpreted in terms of the lowering of the ionization potential of the electron donor.

In the region, 24000—47000 cm^{-1}, the para-substituted *N,N*-dimethylanilines show four bands of CT or LE character (Figs. 4 and 5). The two lower-lying states are closely located and characterized by CT from *N,N*-

Table 3. Absorption maxima (in cm^{-1}) of some *p*-substituted *N,N*-dimethylanilines, p-$(H_3C)_2N$-C_6H_4-X in cyclohexane

X	CT band	LE band
CN	35710	31000—35000[a]
$COCH_3$	31750	
CHO	31250	
NO_2	28170	31000—34000[b]

a) A weak structured band overlapped by the CT band. b) A broad shoulder at the shorter wavelength side of the CT band.

dimethylaniline to the acceptor substituent and also by LE corresponding to $^1B_2 \leftarrow {}^1A_1$ of *N,N*-dimethylaniline. From the absorption maxima of the para-substituted *N,N*-dimethylanilines (Table 3), we can see that the red-shift of the intense CT band is associated with the increase in the electron affinity of the acceptor substituent and the resultant increase in the CT character in S_1. The transition energies of the LE bands seem to remain unchanged by replacing the substituent on the para position. Thus we can expect that the reversal occurs in the order of the two lower-lying states by changing the acceptor substituent group: in cyclohexane, the S_1 state of the cyanoaniline is of LE, while the S_1 state of the nitroaniline is of CT. The reversal is also observed by changing solvents. In nonpolar solvents, the lowest excited singlet state of the cyano-substituted aniline is mainly of LE character, and a reversal of the order of the two lower-lying states occurs by replacing a nonpolar solvent, cyclohexane by polar solvents, such as acetonitrile, ethanol, water, and HFP. Concerning carbonyl-substituted *N,N*-dimethylanilines in the nonpolar solvents the weak LE band is located slightly above the strong CT band and cannot be discernible, while it can be observed separately in HFP.

Table 4. Wave numbers of $T_n \leftarrow T_1$ transitions, ν_{max}, S-T separations, $\Delta\nu_{ST}$, and phosphorescence lifetimes, τ_p for *p*-substituted *N,N*-dimethylanilines, p-$(H_3C)_2N$-C_6H_4-X

X	$\nu_{max}(cm^{-1})$	$\Delta\nu(cm^{-1})$	$\tau_p(s)$
CN	25000[a]	6450[c]	2.16 ± 0.02[c]
$COOCH_3$	24300[d] 23000		
$COCH_3$	22300[a]	4800[b]	0.62 ± 0.02[b]
CHO	22600[a]	4600[b]	0.25 ± 0.01[b]
NO_2	19400[a]	3750[e]	0.22 ± 0.02[e]

a) This work, in ethanol at room temperature. b) This work, in EPA (5:5:2) at 77 K. c) Ref. 36, in EPA (5:5:2) at 77 K. d) Ref. 37, in ethanol at 93 K. e) Ref. 38, in EPA (5:5:2) at 77 K.

The wave numbers of the $T_n \leftarrow T_1$ transitions, the values of S-T separation, and the phosphorescence lifetimes are given in Table 4 for various para-substituted *N,N*-dimethylanilines. The lifetime data indicate that the lowest excited triplet states are of $\pi\pi^*$ character. Since each CT triplet state has the same energy as the corresponding CT singlet state in the zero differential overlap approximation, the decrease of S-T splitting values shows clearly the increase of the CT character in T_1. The increasing CT character in T_1, reflecting the order of the electron affinity of the acceptor substituent, is parallel to the red-shift of the $T_n \leftarrow T_1$ transitions. The decrease of the phosphorescence lifetimes can be qualitatively interpreted in terms of the enhancement of spin-orbit coupling by the intramolecular CT interaction in the same manner as in anilines.[39-41]

We wish to thank Dr. Kazuo Shibata and Dr. Yorinao Inoue, The Institute of Physical and Chemical Research, for their kindness in putting the spectrofluorometer (Shimadzu RF-502) at our disposal.

References

1) S. Nagakura and J. Tanaka, *J. Chem. Phys.*, **22**, 236 (1954).
2) S. Nagakura, *J. Chem. Phys.*, **23**, 1441, (1955).
3) H. C. Longuet-Higgins and J. N. Murrell, *Proc. Phys. Soc.*, **A68**, 601 (1955); J. N. Murrell, *Proc. Phys. Soc., A*, **68**, 969 (1955).
4) J. Tanaka and S. Nagakura, *J. Chem. Phys.*, **24**, 1274, (1956).
5) S. Nagakura, *Mol. Phys.*, **3**, 105, 152 (1960).
6) S. Nagakura, *Pure Appl. Chem.*, **7**, 79 (1960).
7) J. Tanaka, *Bull. Chem. Soc. Jpn.*, **36**, 833 (1963).
8) S. Nagakura, M. Kojima, and Y. Maruyama, *J. Mol. Spectrosc.*, **13**, 174 (1964); K. Tabei, and S. Nagakura, *Bull. Chem. Soc. Jpn.*, **38**, 965 (1965).
9) K. Kimura and S. Nagakura, *Mol. Phys.*, **9**, 117 (1965).
10) H. H. Jaffé and M. Orchin, "Theory and Applications of Ultraviolet Spectroscopy," John Wiley & Sons, Inc., New York (1962) p. 256.
11) J. N. Murrell, "The Theory of the Electronic Spectra of Organic Molecules," Methuen, London (1963).
12) H. Suzuki, "Electronic Absorption Spectra and Geometry of Organic Molecules," Academic Press, New York (1967).
13) C. J. Seliskar, O. S. Khalil, and S. P. McGlynn, "Excited States" ed by E. C. Lim., Academic Press, New York (1974), Vol. 1, p. 231.
14) J. N. Murrell, *Tetrahedron*, **19**, Suppl. 2, 277 (1963); M. Godfrey and J. N. Murrell, *Proc. R. Soc.* London, *Ser. A*, **278**, 69 (1964).
15) R. Grinter and E. Heilbronner, *Helv. Chim. Acta*, **45**, 2496 (1962).
16) Y. H. Lui and S. P. McGlynn, *J. Mol. Spectrosc.*, **55**, 163 (1975).
17) Y. H. Lui and S. P. McGlynn, *J. Lumin.*, **9**, 449 (1975); *ibid.*, **10**, 113 (1975).
18) O. S. Khalil and S. P. McGlynn, *J. Lumin.*, **11**. 185 (1975/76).
19) K. Kimura, *Mol. Phys.*, **15**, 109 (1968).
20) H. Morita, S. Matsumoto, and S. Nagakura, *Bull. Chem. Soc. Jpn.*, **48**, 420 (1975).
21) H. Rupe, A. Braun, and K. von Zembrzuski, *Ber.*, **34**, 3522 (1901).
22) D. E. Pearson and J. D. Burton, *J. Am. Chem. Soc.*, **73**, 864 (1951).
23) H. W. Bresler, W. H. Friedemann, and J. Mai, *Ber.*, **39**, 876 (1906).
24) I. B. Berlman, "Handbook of Fluorescence Spectra of Aromatic Molecules," 2nd ed, Academic Press, New York (1971), p. 291.

25) R, Nakagaki, T. Kobayashi, J. Nakamura, and S. Nagakura, *Bull. Chem. Soc. Jpn.*, **50**, 1909 (1977).
26) T. Kobayashi, S. Matsumoto, and S. Nagakura, *Chem. Lett.*, **1975**, 235.
27) K. Kimura and M. Kubo, *J. Chem. Phys.*, **32**, 1776 (1960).
28) M. Haisa, S. Kishino, T. Yuasa, and K. Akigawa, *Acta Crystallogr., Sect B*, **32**, 1326 (1976).
29) R. Parieser and R. G. Parr, *J. Chem. Phys.*, **21**, 466, 767 (1953).
30) J. Tanaka, *Nippon Kagaku Zasshi*, **78**, 1636 (1957).
31) J. P. Maier and D. W. Turner, *J. Chem. Soc., Faraday Trans. 2*, **1973**, 521.
32) T. Kobayashi and S. Nagakura, *Bull. Chem. Soc. Jpn.*, **47**, 2563 (1974).
33) J. A. Pople, *Proc. Phys. Soc., A*, **68**, 81 (1955).
34) A. Kuboyama, Y. Sato, and H. Arano, *Bull. Chem. Soc. Jpn.*, **49**, 3685 (1976).
35) H. Labhart and G. Wagniere, *Helv. Chim. Acta*, **46**, 1314 (1963).
36) O. S. Khalil, R. H. Hofeldt, and S. P. McGlynn, *Spectrosc. Lett.*, **6**, 147 (1973).
37) I. A. Zhmyreva, V. P. Kolobkov, and S. V. Volkov, *Opt. Spectrosc.*, **20**, 162 (1966).
38) O. S. Khalil, C. J. Seliskar, and S. P. McGlynn, *J. Chem. Phys.*, **58**, 1607 (1973).
39) E. C. Lim and S. K. Chakrabarti, *Chem. Phys. Lett.*, **1**, 28 (1967).
40) E. C. Lim and S. K. Chakrabarti, *J. Chem. Phys.*, **47**, 4726 (1967).
41) M. Kasha and H. R. Rawls, *Photochem. Photobiol.*, **7**, 561 (1968).